link to online abstract
https://doi.org/10.1364/oe.541946

Research Article Vol. 32, No. 24 / 18 Nov 2024 / Optics Express 43635
Optics EXPRESS

Femtosecond Mamyshev fiber oscillator started by ultra-low power microchip laser seeder at two different wavelengths: a comparison

RICCARDO GOTTI,[1,*] SARA PIZZURRO,[1] FRANCESCO CANELLA,[2] DARIO GIANNOTTI,[3] GIANLUCA GALZERANO,[2] ANTONIO AGNESI,[1,4] AND FEDERICO PIRZIO[1]

[1]*Dipartimento di Ingegneria Industriale e dell'Informazione, Università di Pavia, Via Ferrata 5, 27110 Pavia, Italy*
[2]*Istituto di Fotonica e Nanotecnologie - Consiglio Nazionale delle Ricerche, 20133 Milano, Italy*
[3]*Dipartimento di Fisica, Politecnico di Milano, 20133 Milano, Italy*
[4]*Bright Solutions Srl, Via degli Artigiani 27, 27010 Cura Carpignano, Italy*
[*]*riccardo.gotti@unipv.it*

Abstract: A 1-W average output power, sub-60-fs femtosecond Mamyshev fiber oscillator was reliably started by a passively Q-switched sub-ns microchip laser generating four-wave-mixing signals in a polarization-maintaining passive fiber, at either 1064 nm or at 1033 nm. We show experimentally that seeding at 1033 nm provides much higher quality pulses with a duration as short as 41 fs and minimal satellites. The evolution toward the gain-managed nonlinear amplification regime clearly takes place when seeding the oscillator closer to the peak gain of the Yb-doped fiber.

1. Introduction

Ultrafast Mamyshev fiber laser oscillators attracted significant interest in the last decade, owing to their ability to sustain pulses with very large nonlinear phase ~100π and compressible down to ~40 fs with excellent quality [1–4]. To initiate the pulse formation eventually evolving to a stable mode-locking regime, either pump power modulation [1,5] or seeding with an external source [2,6,7] were mostly employed. In the second case, a compact low-cost sub-ns 1064-nm microchip solid-state laser was demonstrated as a convenient device to efficiently start an Yb-fiber Mamyshev oscillator even with a single seeding pulse, both in the low-power and high-power level pumping regime [8,9].

In this work we extend this technique showing that seeding a Yb-fiber Mamyshev oscillator at ~1030 nm significantly improves the quality of the generated pulse trains. This is possible thanks to the evolution toward the gain-managed nonlinear amplification (GMNA) regime that was identified [10] as an extension of the parabolic self-similar amplification [11] beyond the Yb^{3+}-fiber gain bandwidth, leading to the generation of sub-40-fs pulses up to microjoule energy with large mode area fiber amplifiers [12]. For the seed source, we employed a passively Q-switched (PQS) sub-nanosecond microchip laser operating at 1064 nm, coupled to a few meters of polarization-maintaining (PM) fiber. This setup generates wavelength pairs around 1064 ± 30 nm through the degenerate four-wave mixing (DFWM) process. A particular seed wavelength can be easily selected using spectral filtering before entering the oscillator. Despite the modest conversion efficiency (fraction of percent), the extremely low (few hundreds of pJ) seeding pulse energy at 1033 nm required to trigger the oscillation in the Mamyshev regenerator can be readily obtained using ~kW peak-power sub-ns pulses at 1064 nm.

#541946 https://doi.org/10.1364/OE.541946
Journal © 2024 Received 11 Sep 2024; revised 12 Oct 2024; accepted 12 Oct 2024; published 15 Nov 2024

Optics EXPRESS

The aim of the present investigation is to provide a detailed comparison of the laser pulse spectrum evolution and pulse duration when seeding the Mamyshev oscillator at 1033 nm and 1064 nm. GMNA performance was recently studied in [13,14], where an amplifier was seeded at different wavelengths, demonstrating that better pulse quality is achieved when seeding near 1026 nm compared to 1037 nm. Our findings are consistent with those results, even for a GMNA within a Mamyshev oscillator seeded at different wavelengths. Experimentally, in both seeding cases the oscillator performance reaches a level close to the state of the art in terms of compressed pulse duration, average and peak power, but we clearly show the differences between the two final regimes. In particular, the pulse-to-pedestal energy ratio (sometimes a Strehl ratio is defined) is drastically improved in the first case, leading to almost pedestal-free 41-fs pulse with 0.75-W average output power, after a 75% efficiency compressor, at 12-MHz repetition rate and a more than two-fold improvement in the pulse peak power reaching 1.5 MW after compression.

2. Experimental setup and seeder characterization

The setup of the ring Mamyshev oscillator is shown in Fig. 1. The active fiber DC-F is a 4-m long Yb-doped double-clad (DC) fiber (n-LIGHT Yb1200-10/125DC) pumped by a 5-W fiber-coupled laser diode (PLD) emitting at 976 nm (NA = 0.22, core diameter 105 µm) with a coupling efficiency of ~70%. F1 is a commercial multilayer bandpass sharp-edges super-gaussian filter (Semrock LL01-1064) which can be angle-tuned to have its transmission bandwidth of ~3.5 nm full width at half maximum (FWHM) centered either at ~1060 nm or at ~1030 nm, depending on the seeding wavelength. The reflection from F1 also works as the output coupling for the laser. The transmitted portion from F1 is coupled in a 12-m-long PM single-mode fiber (PM-980-XP), acting as the passive arm of the oscillator [9], with a coupling efficiency of ~60%. The output of the passive fiber is filtered by filter F2, which is realized by the combination of a reflective diffraction grating (Thorlabs GR13-0610) with 600 grooves/mm and the successive coupling into the fiber amplifier. The spectral profile of such a filter is approximately Gaussian with a measured bandwidth of ~1.5-nm FWHM. By adjusting the angle of incidence on the grating, the peak transmission wavelength of F2 can be readily tuned in the range of interest, 1030-1070 nm. An optical isolator is included in the ring to make it unidirectional, thus preventing potentially harming effects such as Brillouin scattering. To avoid the continuous-wave lasing of the ring cavity, the transmission windows of F1 and F2 are separated by ~10 nm, close to the selected seeding wavelength.

A diode-pumped PQS Nd/Cr:YAG microchip laser at 1064 nm (Bright Solutions srl) was employed as the seeder to start the mode-locking regime in the oscillator, like in our previous work [8]. The use of picosecond-long pulses (either mode-locked lasers or gain-switched diodes) to initiate the generation of ultrashort pulses is a well-established concept, as reported in [15], for example. However, our seeder provides much longer 400-ps, single longitudinal mode, linearly polarized pulses with an energy of ~2 µJ. A 5-m-long PM panda fiber (PM-980-XP model) was chosen to transfer sufficient energy into the DFWM band at the seeding wavelengths. Birefringent phase-matching is known to provide a means to generate a pair of equally spaced optical frequencies (signal and idler) around the pump wavelength [16,17]. Assuming a birefringence value $\delta n \sim 2.7\times10^{-4}$, in fair agreement with the value implied by the beat length for the PM-980-XP fiber employed (Thorlabs, Inc.), a pump wavelength λ_p of 1064 nm, and the fused silica dispersion k_p''~17 fs^2/mm, a wavelength shift:

$$\Delta\lambda = \frac{\lambda_p^2 \delta n}{2\pi c^2 k_p''} \sim 30 \text{ nm}$$

is predicted assuming the pump polarized at 45° with respect to a fiber axis, with signal and idler polarized along the fast- and slow-axis, respectively. Figure 2.a and the insets show the measured

Optics EXPRESS

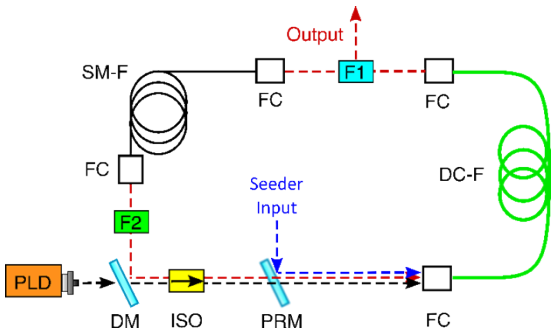

Fig. 1. Setup of the ring oscillator. PLD: 5-W pump laser diode. DM: dichroic mirror. ISO: optical isolator, range 1030-1080 nm, 4 mm aperture, (Electro-Optics Technology Inc.). PRM: partially reflective dielectric mirror (R = 10%). FC: fiber collimator. DC-F: 4-m long Yb-doped fiber amplifier. SM-F: single-mode PM passive fiber. F1: angle-tuned super-gaussian filter. F2: 600 grooves/mm reflective grating. The seeder input wavelength at PRM may be selected to be 1032 nm or 1064 nm: the oscillation starts accordingly at those central wavelengths after adjusting the transmission windows of F1 and F2.

DFWM spectrum of the seeder and corresponding shifted peaks at ~1033 nm (signal) and ~1098 nm (idler), for different PQS pulse energy coupled in the PM fiber. At an incident PQS pulse energy of ~700 nJ, the broadband frequency shifted signal and idler pulses start to emerge from the noise floor of the optical spectrum analyzer (Yokogawa model ANDO-AQ6317B). At this pump pulse level, non-phase-matched DFWM is not yet significantly broadening the spectrum around the pump (1064 nm), signal (1033 nm) and idler (1098 nm) peaks. By increasing the pump pulse energy, we observe the progressive growth and broadening of the sidebands at each wavelength to as much as a few nanometers, which is crucial to provide initial noise fluctuation intense enough to start the mode-locking regime in the Mamyshev oscillator, as outlined in [8]. A 6-GHz oscilloscope (Tektronix TDS6604B) with a 70-ps rise-time photodiode, shows the signal and idler pulses significantly shorter than the pump ones, down to ~150 ps duration.

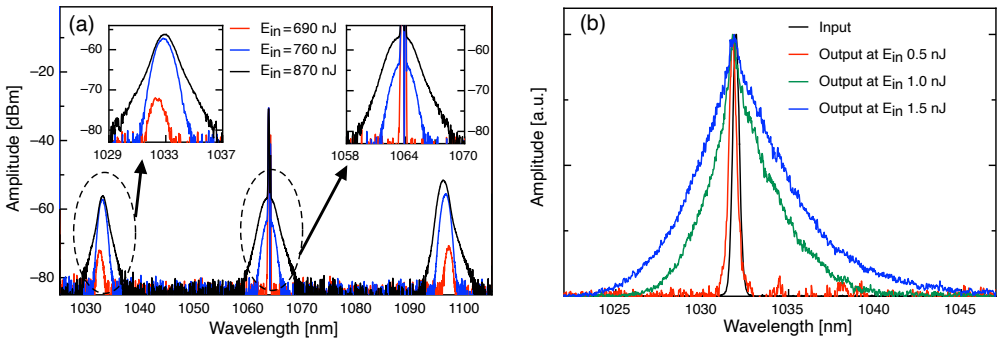

Fig. 2. (a) DFWM spectrum of the PQS microchip seeder for different coupled energies in a 5-m long single-mode PM passive fiber. In the insets are shown close view around 1033 nm and around 1064 nm. (b) Open-ring broadening of the seeder DFWM-filtered spectrum at 1033 nm, at the output of the Yb-doped DC amplifier before being transmitted through the filter F1 in the passive arm. Here the vertical scale is linear and normalized to 1 at the peak. For input energy above 1 nJ at 1033 nm, at an incident pump power in the active fiber of 2.5 W, the Mamyshev oscillator can be started reliably.

Optics EXPRESS

By using at the output of the PM fiber a second sharp-edge passband filter identical to F1, either the non-phase matched DFWM broadened portion of the spectrum around the pump at 1064 nm or the signal at 1033 nm could be selected for seeding the Mamyshev oscillator. Experimentally, we found that injecting the oscillator with energy as low as 200 pJ for the filtered seeder spectrum around 1033 nm or 1064 nm was sufficient to reliably start the mode-locking when the incident pump power in the active fiber is 2.5 W, corresponding to the threshold of the mode-locking regime.

With our experimental setup, we found an alternative method to initiate Mamyshev oscillation by directly injecting the narrowband pulse at ~1033 nm (black curve in Fig. 2(b)), without any additional FWM broadening. Then the spectrum broadens naturally within the fiber amplifier.

Figure 2.b shows the spectral broadening of the seeder spectrum, taking place directly in the DC active fiber of the ring oscillator pumped at 2.5 W, for different values of input energy at 1032 nm. In this measurement, the ring was "open" since the effect of amplification on the seed pulse needed to be investigated without the circulating mode-locking pulse (the same situation as at the starting event of the mode-locking dynamics). Above 1-nJ of signal pulse energy, the non-phase-matched DFWM broadening occurring in the fiber amplifier is sufficient to reliably trigger the mode-locking in the Mamyshev oscillator. As shown in Ref. [9], seeder energy above 1 nJ over a spectral bandwidth of about 10 nm exceeds by more than one order of magnitude the amplified spontaneous emission energy contained in the seeder pulse duration.

3. Mode-locking results

Figure 3.a shows the oscillator output power as a function of the incident pump power, for the seeding wavelengths of 1033 nm (blue curves) and 1064 nm (red curves). At 4.5-W incident pump power, in both cases, the average output power reaches 1 W before pulse compression, with different slope efficiencies of 40% and 30%, respectively, due to the higher gain of the DC active fiber when seeded around 1030 nm. Figure 3.b reports the spectral bandwidths (right scale) for different incident pump powers and corresponding pulse durations (left scale) after compression using a folded Treacy grating compressor [18] (transmission grating with 600 grooves/mm) with more than 75% total efficiency. The negative second order dispersion provided by the compressor, to minimize the duration starting from values in the range 3-5 ps, is around -6×10^4 fs^2 and -9×10^4 fs^2 for the shortest pulse when seeding at 1033 nm and 1064 nm respectively.

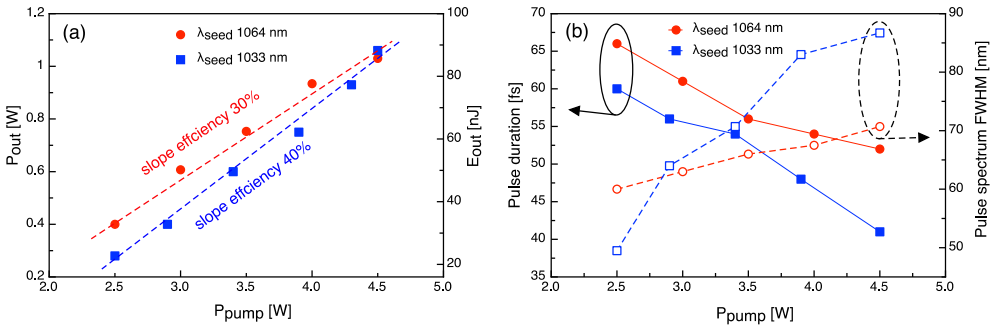

Fig. 3. (a) Mamyshev oscillator average output power and pulse energy as a function of the incident pump power for seeding wavelength 1064 nm, in red, and 1033 nm, in blue, with corresponding slope efficiencies. (b) Compressed pulse durations (solid lines, left scale) and full width at half maximum (FWHM) spectral widths (dashed lines, right scale) for 1064 nm (red) and 1033 nm (blue) seeding wavelength.

The behavior of the Mamyshev oscillator is significantly different when seeded at 1064 or 1033 nm. This is evident when we analyze both the evolution of the spectrum (see Fig. 4) and the

Optics EXPRESS

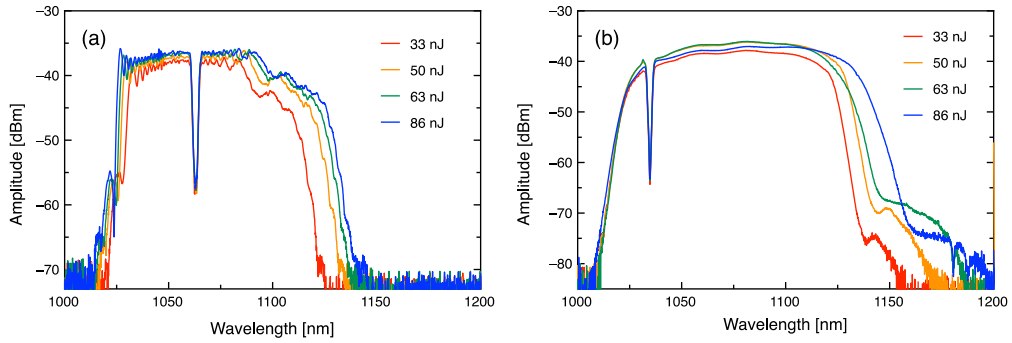

Fig. 4. Mamyshev oscillator output spectrum evolution for different output pulse energy, (a) for the case of 1064-nm and (b) 1033-nm injection. Remarkably, by using the same seeding technique in both cases, the distinctive features of the GMNA regime are present only for injection at 1033 nm.

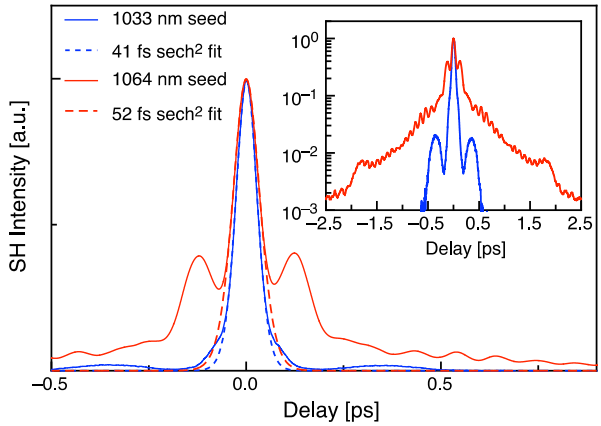

Fig. 5. Second-harmonic intensity autocorrelations after compression for the shortest pulses in case of 1064-nm seed injection (red curves, 52-fs pulse duration of the main peak) or 1033 nm seed injection (blue curve, 41-fs pulse duration). The vertical scale is linear and normalized to 1 at the peak. In the inset we show the AC traces in the vertical axis log scale for a better comparison of the pulse pedestals on the full AC delay line span.

non-collinear second harmonic autocorrelation (SHAC) traces after compression (see Fig. 5), measured with a commercial autocorrelator (A.P.E. model pulseCheck-50-NX).

Comparing the spectral evolution for the seeding wavelengths with the dynamics outlined in Ref. [19] it is clear that seeding at 1064 nm produces an incomplete evolution toward the GMNA regime which is known, instead, to yield high-quality compressible pulses with monotonic chirp, matching the grating compressor phase [10]. Indeed, in this case the spectrum is shown to widen progressively also on the blue side of the seed wavelength (the Mamyshev offset filters are relatively close to the seed wavelength, being their separation limited to ~10 nm). The compressed pulse at the maximum pump power shows evident multiple satellites contribution (see Fig. 5) just like in Ref. [19], middle-way toward the final broad spectrum supporting a clean single pulse before the perturbing Raman effect sets in.

This is in sharp contrast with the GMNA well-known evolution, where the spectrum initially broadens symmetrically, then after the blue-side meets the absorption edge of the Yb^{3+} ion the center of mass of the spectrum starts to redshift, until exceeding the gain bandwidth of the fiber

Optics EXPRESS

amplifier [10,12]. Spectral broadening stops when the Raman resonance at ~1150 nm is reached, ultimately affecting the coherence of the generated pulse. Besides the significant redshift, which is a key feature of this regime, the GMNA spectrum is smoother and characterized by sharper edges. This is exactly what happens when seeding at 1033 nm. Mamyshev offset filters are now located around this wavelength: the spectrum evolution starts much closer to the absorption edge and clearly evolves towards the GMNA regime within the pulse energy range available, before the disruption of mode-locking due to Raman onset. This results in superior quality of the compressed pulses along with a significant reduction of the minimum pulse duration from ~50 fs to ~40 fs when seeding at 1064 nm and 1033 nm, respectively. In this latter case, the AC trace (see Fig. 5) clearly shows the presence of only a single residual satellite pulse with an amplitude of the order of 2% with respect to the main pulse.

Table 1 summarizes the measurements of pulse duration, average output power after compression and percentage of energy in the main peak of the SHAC traces of the compressed pulses for the two different seeding conditions. For increasing pump power, the minimum pulse duration progressively reduces in both cases approaching the 40-fs limit for the 1033-nm seeding and the 50-fs limit for the 1064-nm seeding. However, in the latter case a strong pedestal (see Fig. 5) impairs the final pulse quality limiting the energy fraction of the main peak to about 34%. This behavior is similar to what was observed by Ye et al. in Ref.s [13,14], where seeding a GMNA with pulses centered around 1024 nm resulted in better pulse quality compared to seeding around 1037 nm. With respect to our previous experiments [9], here we optimized the spectral filter separation only at the mode-locking threshold and did not adjust it to optimize the compressed pulse quality while increasing the pump power. This resulted in a progressive reduction of the energy in the main lobe of the SHAC trace (see Table 1). This behavior is in stark contrast to what we observe when seeding at 1033 nm. In this case, the pulse quality is already very good close to the mode-locking threshold and progressively improves to a maximum of 85% of the energy in the main peak of the SHAC. Since, for non-overlapping main and small satellite pulses, the satellite content is one half of the SHAC background, we can estimate that at least 92% of the energy is in the main pulse.

Table 1. The compressed pulse duration is calculated from the best fit of the main lobe of the experimental second-harmonic intensity AC for seeding at 1064 nm and at 1033 nm. The percentage of energy in the main pulse is obtained from the ratio of the area of the main lobe and the total area of the AC trace.

Seeding wavelength	1064 nm			1033 nm		
Incident pump power	**Compressed pulse duration**	**Average power after compression**	**Area % of the main AC peak**	**Compressed pulse duration**	**Average power after compression**	**Area % of the main AC peak**
3.0 W	61 fs	455 mW	39%	56 fs	325 mW	77%
3.5 W	56 fs	565 mW	37%	54 fs	450 mW	87%
4.0 W	54 fs	700 mW	35%	48 fs	625 mW	84%
4.5 W	52 fs	770 mW	34%	41 fs	795 mW	85%

This is confirmed by a SHG-FROG measurement (available as an option with the same autocorrelator model) carried out on the pulses when seeding at 1033 nm at 4.5 W incident pump power and presented in Fig. 6. The retrieved pulse spectrum (see Fig. 6.c) is in fairly good agreement with the measured spectrum and shows a spectral phase almost flat across 1040-1110 nm. The retrieved pulse (see Fig. 6.d) presents a single satellite accounting for about 6% of the total pulse energy from numerical integration in very good agreement with the estimations based on the measurement of the SHAC background.

Optics EXPRESS

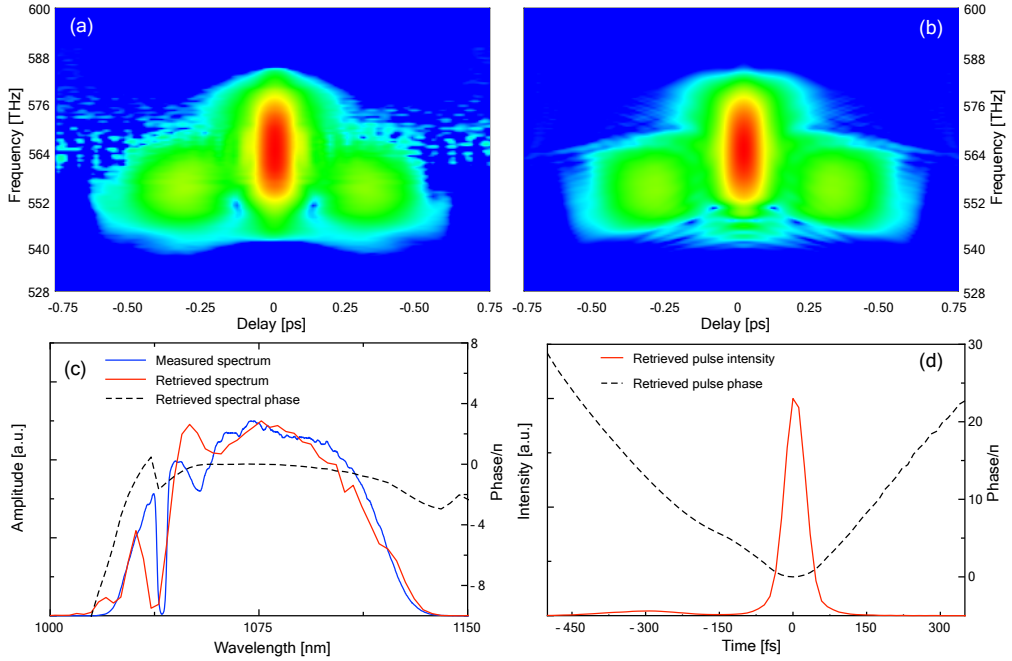

Fig. 6. (a) Measured SHG-FROG trace. (b) Retrieved SHG-FROG trace with 0.0035 error on a 128×128 grid. (c) Pulse optical spectrum (blue line) and retrieved optical spectrum (red line). The retrieved spectral phase in units of π is shown in black dashed line. (d) Retrieved pulse temporal intensity profile and temporal phase in units of π showing the pulse satellite accounting for 6% of the total pulse energy from numerical integration. The vertical scales on the left of 6.(c) and 6.(d) are linear and normalized to 1 at the peak.

At the maximum incident pump power, for injection at 1033 nm, the minimum compressed pulse duration is 41 fs. Given the 86-nJ total energy, considering the 75% compressor efficiency, the final pulse peak power is about 1.5 MW. Seeding at 1033 nm also makes the output pulse quality much more independent from the fine tuning of the spectral filters transmission central wavelength and offset. Furthermore, we notice that seeding at 1033 nm with our technique is also safer and particularly convenient, since the DFWM band is well separated spectrally from the narrowband residual pump, thus making suppression of the latter straightforward, which is mandatory to avoid potential issues in the high-gain fiber amplifier.

4. Conclusions

In conclusion, we presented a 1-W average output power Mamyshev oscillator based on a ring cavity with Yb-doped DC active fiber and started by a simple and cheap 400-ps PQS microchip laser emitting at 1064 nm. By exploiting DFWM in a standard single-mode polarization maintaining fiber, it is possible to generate sub-ns seeding pulses at 1033 nm which proved much more effective to trigger the mode-locking regime. We provide a direct comparison of the spectrum evolution when seeding the oscillator at 1033 nm and 1064 nm, clearly showing substantially different final regimes in these two cases. Seeding the oscillator at 1033 nm close to the absorption edge of the Yb^{3+} ion forces the laser to reach more effectively the GMNA regime. In stark contrast when seeding at 1064 nm such a regime is not reached in our oscillator, strongly hampering its performance and pulse quality. In particular, the pulse pedestal content is

Optics EXPRESS

significantly reduced for injection at 1033 nm, leading to 41-fs pulses well exceeding the 1-MW level of peak power after compression in a standard Treacy grating compressor.

The proposed Mamyshev seeder/oscillator architecture can be further integrated with commercial fiber components to make the laser system even more compact and user-friendly, which was not the purpose of the present investigation.

Funding. ATTILA - Advanced room-Temperature THz hyperspectral Imagin based on novel ultrafast fiber LAsers (20227849RL); Integrated infrastructure initiative in PHOtonic and Quantum Sciences (IR0000016).

Acknowledgments. The authors are grateful to Dr. Cristian Manzoni for the fruitful discussions and his help with the FROG measurements.

The authors acknowledge financial support by the European Union's NextGenerationEU Programme with the I-PHOQS Infrastructure [IR0000016, ID D2B8D520, CUP B53C22001750006] Integrated infrastructure initiative in PHOtonic and Quantum Sciences.

Disclosures. The authors declare no conflicts of interest.

Data availability. Data underlying the results presented in this paper are not publicly available at this time but may be obtained from the authors upon reasonable request.

References

1. H. Haig, P. Sidorenko, R. Thorne, *et al.*, "Megawatt pulses from an all-fiber and self-starting femtosecond oscillator," Opt. Lett. **47**(4), 762–765 (2022).
2. P. Repgen, D. Wandt, U. Morgner, *et al.*, "Sub-50 fs, µJ-level pulses from a Mamyshev oscillator–amplifier system," Opt. Lett. **44**(24), 5973–5976 (2019).
3. V. Boulanger, M. Olivier, F. Guilbert-Savary, *et al.*, "All-fiber Mamyshev oscillator enabled by chirped fiber Bragg gratings," Opt. Lett. **45**(12), 3317–3320 (2020).
4. V. Boulanger, M. Olivier, F. Trépanier, *et al.*, "Multi-megawatt pulses at 50 MHz from a single-pump Mamyshev oscillator gain-managed amplifier laser," Opt. Lett. **48**(10), 2700–2703 (2023).
5. I. Samartsev, A. Bordenyuk, and V. Gapontsev, "Environmentally stable seed source for high power ultrafast laser," Proc. SPIE **10085**, 100850S (2017).
6. K. Regelskis, J. Želudevičius, K. Viskontas, *et al.*, "Ytterbium-doped fiber ultrashort pulse generator based on self-phase modulation and alternating spectral filtering," Opt. Lett. **40**(22), 5255–5258 (2015).
7. Z. Liu, Z. M. Ziegler, L. G. Wright, *et al.*, "Megawatt peak power from a Mamyshev oscillator," Optica **4**(6), 649–654 (2017).
8. S. Pizzurro, R. Gotti, L. Carrà, *et al.*, "Femtosecond Mamyshev fiber oscillator started by a passively Q-switched microchip laser," Opt. Lett. **47**(8), 1960–1963 (2022).
9. R. Gotti, L. Carrà, S. Pizzurro, *et al.*, "1 MW peak-power Mamyshev oscillator started by a passively Q-switched microchip laser," Adv. Phot. Res. **2400028**, 1 (2024).
10. P. Sidorenko, W. Fu, and F. Wise, "Nonlinear ultrafast fiber amplifiers beyond the gain-narrowing limit," Optica **6**(10), 1328–1333 (2019).
11. M. E. Fermann, V. I. Kruglov, B.C. Thomsen, *et al.*, "Self-Similar Propagation and Amplification of Parabolic Pulses in Optical Fibers," Phys. Rev. Lett. **84**(26), 6010–6013 (2000).
12. P. Sidorenko and F. Wise, "Generation of 1 µJ and 40 fs pulses from a large mode area gain-managed nonlinear amplifier," Opt. Lett. **45**(14), 4084–4087 (2020).
13. H. Ye, L. Pontagnier, E. Cormier, *et al.*, "Multi-gigahertz femtosecond pulses from linear and nonlinear propagation of a phase-modulated laser," Opt. Lett. **47**(20), 5405–5408 (2022).
14. H. Ye, L. Pontagnier, E. Cormier, *et al.*, "Supplementary document for "Multi-GHz femtosecond pulses from linear and non-linear propagation of a phase-modulated laser"," Optica Publishing Group, Journal contribution, https://doi.org/10.6084/m9.figshare.21206183.v2.
15. W. Fu, L.G. Wright, and F.W. Wise, "High-power femtosecond pulses without a modelocked laser," Optica **4**(7), 831–834 (2017).
16. G. P. Agrawal, *Nonlinear fiber optics*, Springer, Berlin Heidelberg (2000).
17. R. H. Stolen, M. A. Bösch, and Chinlon Lin, "Phase matching in birefringent fibers," Opt. Lett. **6**(5), 213–215 (1981).
18. V. Chauhan, P. Bowlan, J. Cohen, *et al.*, "Single-diffraction-grating and grism pulse compressors," J. Opt. Soc. Am. B **27**(4), 619–624 (2010).
19. D. Tomaszewska-Rolla, R. Lindberg, V. Pasiskevicius, *et al.*, "A comparative study of an Yb-doped fiber gain-managed nonlinear amplifier seeded by femtosecond fiber lasers," Sci. Rep. **12**(1), 404 (2022).